

UC Santa Barbara

UC Santa Barbara Previously Published Works

Title

Programmable, Multiplexed DNA Circuits Supporting Clinically Relevant, Electrochemical Antibody Detection

Permalink

<https://escholarship.org/uc/item/0sv4p4np>

Journal

ACS Sensors, 6(6)

ISSN

2379-3694

Authors

Bracaglia, Sara
Ranallo, Simona
Plaxco, Kevin W
et al.

Publication Date

2021-06-25

DOI

10.1021/acssensors.1c00790

Peer reviewed

Programmable, Multiplexed DNA Circuits Supporting Clinically Relevant, Electrochemical Antibody Detection

Sara Bracaglia, Simona Ranallo,* Kevin W. Plaxco, and Francesco Ricci*

Cite This: *ACS Sens.* 2021, 6, 2442–2448

Read Online

ACCESS |



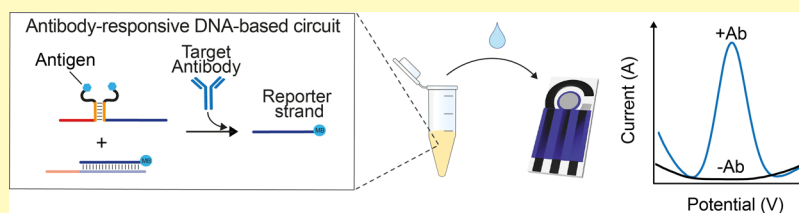
Metrics & More



Article Recommendations



Supporting Information



ABSTRACT: Current health emergencies have highlighted the need to have rapid, sensitive, and convenient platforms for the detection of specific antibodies. In response, we report here the design of an electrochemical DNA circuit that responds quantitatively to multiple specific antibodies. The approach employs synthetic antigen-conjugated nucleic acid strands that are rationally designed to induce a strand displacement reaction and release a redox reporter-modified strand upon the recognition of a specific target antibody. The approach is sensitive (low nanomolar detection limit), specific (no signal is observed in the presence of non-targeted antibodies), and selective (the platform can be employed in complex media, including 90% serum). The programmable nature of the strand displacement circuit makes it also versatile, and we demonstrate here the detection of five different antibodies, including three of which are clinically relevant. Using different redox reporters, we also show that the antibody-responsive circuit can be multiplexed and responds to different antibodies in the same solution without crosstalk.

KEYWORDS: DNA nanotechnology, electrochemical biosensors, antibody monitoring, DNA circuits, DNA sensors

The COVID19 pandemic has highlighted the crucial role that diagnostic tests can play in the detection, monitoring, and containment of infectious diseases.^{1,2} Different biomarkers can be used for such monitoring, but antibodies are among the most important as their detection not only reports on current and past infection but, in the latter case, also can inform on clinical outcomes.^{3,4} Antibody detection is likewise important in the treatment and monitoring of autoimmune diseases and cancer^{5,6} and, as antibodies are increasingly employed as therapeutic agents, in therapeutic drug monitoring.^{7–10}

Recent years have seen extensive efforts to develop antibody detection strategies that are not only rapid, inexpensive, and easy to use but also quantitative, sensitive and useable at the point of care.^{11,12} Lateral flow immunoassays, thanks to their ease of use, their low cost, and their ability to work with unprocessed clinical samples, have become the uncontested leaders for antibody detection in point-of-care settings.¹³ Lateral flow assays, however, are usually qualitative, thus preventing their use in applications such as therapeutic monitoring, which requires precise quantitation.^{14,15} From this perspective, the ideal benchmark of an analytical point-of-care device remains without doubt the electrochemical glucose self-monitoring meter being not only quantitative but also cost-effective and easy to use.¹⁶ Electrochemical sensors are particularly well suited for point-of-care applications as they

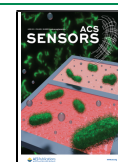
usually work well even when deployed directly in complex sample matrices, require low-cost instrumentation, can be mass-produced, and can be easily multiplexed.¹⁷

Recently, DNA nanotechnology, an emerging research field in which synthetic DNA strands are used to build structures and devices with nanoscale precision, has provided new sensing approaches for the detection of a wide range of targets.^{18–23} Among these methods, the design of DNA-based circuits in which different-responsive DNA synthetic strands react in a programmable way to give an output signal only in the presence of a specific target has given promising results.^{24–27} Several DNA-based circuits,^{28,29} for example, have been reported to date in which the detection of specific biomolecules has been achieved by optical- or colorimetric-based outputs.^{30–33} More recently, the electrochemical detection of specific genes and small molecules using DNA-based circuits has been also proposed.³⁴

Received: April 16, 2021

Accepted: June 3, 2021

Published: June 15, 2021



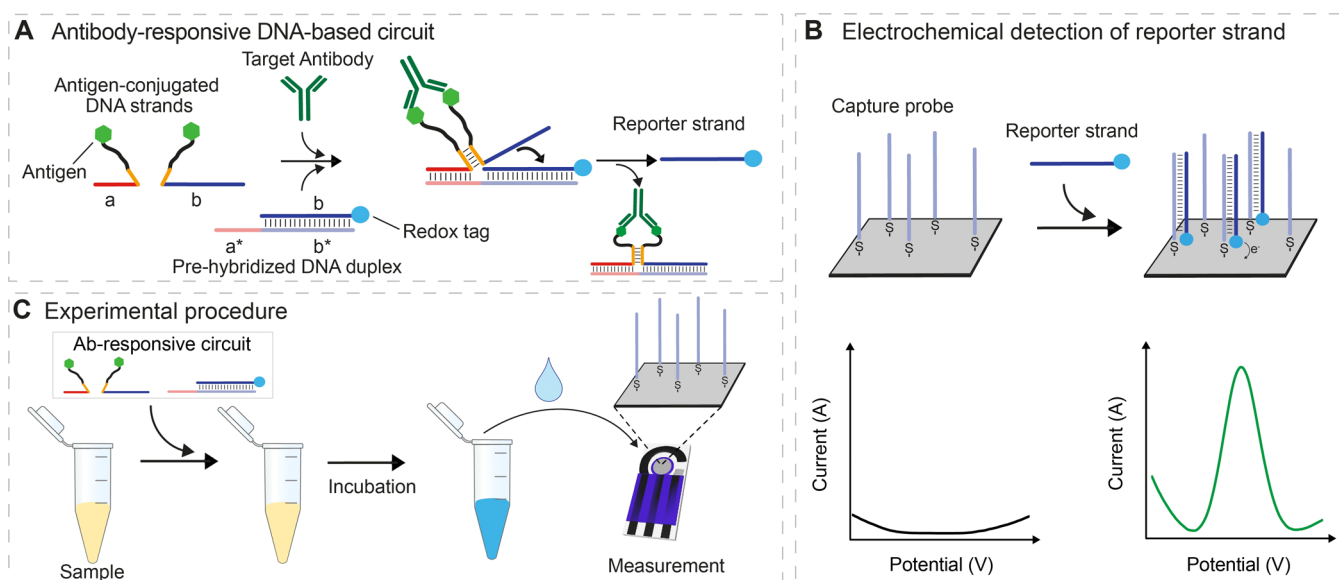


Figure 1. (A) Antibody-responsive nucleic acid circuit is made of a pre-hybridized duplex DNA containing the redox-labeled reporter and of two antigen-conjugated DNA strands. The binding of the target antibody to the two antigen-conjugated strands induces the formation of a functional complex able to activate a strand displacement reaction that releases the redox-labeled reporter strand from the pre-hybridized duplex. (B) Redox-labeled reporter strand can be detected through an electrochemical platform composed of a silver-based screen-printed disposable electrode on which a complementary DNA capture strand is immobilized. The hybridization of the reporter strand leads to a measurable electrochemical signal using square wave voltammetry (SWV). (C) Schematic of the measuring procedure: the antibody-responsive circuit elements are mixed with the sample of interest and incubated at room temperature (RT) and then transferred onto the screen-printed electrode surface for electrochemical measurement.

Motivated by the abovementioned considerations, we propose here the rational design of a DNA-based circuit that can be applied for the quantitative electrochemical detection of multiple, specific antibodies. The platform employs synthetic DNA strands as scaffolds for the conjugation of antibody-responsive elements and electrochemical signaling tags and allows us to couple the advantages of electrochemical detection with those of DNA-based circuits.³⁵

RESULTS

Our approach is based on the use of an antibody-responsive DNA strand displacement reaction (DNA “circuit”)^{28,30} re-engineered so that it can induce the release of a redox reporter-modified DNA strand in the presence of a specific target antibody. By combining such an antibody-responsive circuit with a disposable electrode on which a DNA capture sequence has been immobilized, we can achieve the sensitive and specific electrochemical quantitation of specific antibodies. The antibody-responsive circuit we have developed employs a set of three synthetic elements: a DNA duplex and two antigen-conjugated single-stranded DNAs. The duplex is composed of a 21-base redox reporter-modified strand and a 33-base strand that contains a 21-base fully complementary portion (denoted as “b*” in Figure 1A) but also includes an extra 12-base, single-stranded “toehold” domain (denoted as “a*” in Figure 1A). The two antigen-conjugated strands share a short complementary region (orange) connected to a 12-base poly-T linker (black) that terminates with a covalently attached antigen (Figure 1A). One of these two antigen-conjugated strands also includes a sequence (denoted as “a” in Figure 1A) complementary to the 12-base toehold of the pre-hybridized duplex. The other includes a sequence (denoted as “b” in Figure 1A) complementary to the 21-base strand in the duplex. Bivalent binding of the target antibody to the two antigen-

conjugated DNA strands induces their co-localization, triggering in turn the hybridization of their short complementary regions, which would otherwise not form a duplex (orange, Figure 1A). The resulting complex binds to the toehold portion of the pre-hybridized duplex and invades it, releasing the redox reporter-modified single strand. This then hybridizes to the capture strand attached to the electrode, thus generating an easily measurable electrochemical signal (Figure 1B).

Instrumental for the correct functioning of the circuit is the rational design of antigen-conjugated strands that only hybridize and thus form the complex required to release the reporter strand, upon being brought into proximity via antibody binding. As our design test bed, we first employed the small-molecule hapten digoxigenin (Dig) to target anti-Dig antibodies (Figure 2A). To do this, we designed a series of Dig-conjugated DNA strands differing in the length of their complementary regions, thus forming duplexes of varying stability (orange, Figure 2A). Specifically, we tested lengths ranging from 0 to 14 bases by recording SWVs in the absence and presence of saturating (300 nM) anti-Dig antibodies (Figure 2B). Doing so, we found that complementary regions longer than eight bases are not optimal because they are stable enough to produce measurable electrochemical signals even in the absence of anti-Dig antibodies (Figure S1). Shortening the complementary sequence, however, reduces this background until, at four bases, the background becomes undetectable (i.e., indistinguishable from that of a control construct lacking any complementarity). Bivalent binding of the targeted antibody to the two antigen-conjugated strands, on the other hand, produces measurable signals with complementary regions as short as four nucleotides (Figure S1). The greatest signal change between the absence and presence of the target antibody is achieved with six bases of complementarity

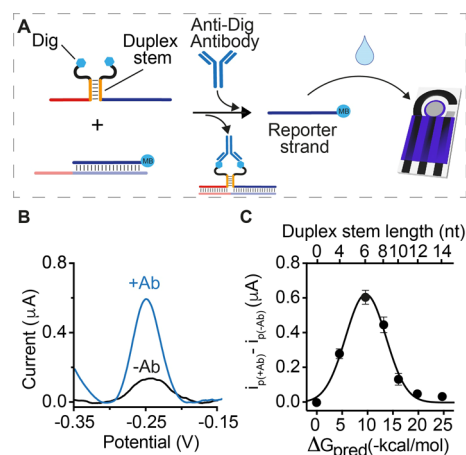


Figure 2. (A) Anti-Dig antibody-responsive circuit was used for signaling optimization. (B) SWV scans obtained in the absence (black) and presence (blue) of anti-Dig antibodies using Dig-conjugated DNA strands with 6-base complementary portions. (C) Plot showing the difference between the electrochemical signals obtained in the presence ($i_{p(+Ab)}$) and absence ($i_{p(-Ab)}$) of anti-Dig antibodies with Dig-conjugated DNA strands with variable lengths of the complementary portions. The experiments were performed in a 100 μ L phosphate buffer solution (50 mM Na_2HPO_4 , 150 mM NaCl, pH 7.0) containing the pre-hybridized DNA duplex (60 nM), Dig-conjugated DNA strands (100 nM each), and anti-Dig antibodies (300 nM). The antibody-responsive circuit was allowed to react for 30 min at RT after antibody addition and then transferred to the disposable electrode surface. SWV scans were performed between -0.35 and -0.15 V at 50 Hz.

between the two antigen-conjugated strands (Figure 2C), and thus, we employed this length in all following experiments.

The optimized antibody-responsive circuit achieves the specific, sensitive, and convenient detection of anti-Dig antibodies in clinically relevant sample matrices. To see this, we challenged the anti-Dig-responsive circuit in antibody-doped, 90% bovine blood serum, a safe and convenient proxy for human samples (Figure 3A). In this matrix, the reaction kinetics is similar to that observed in buffer (Figure S2), and the limit of detection (defined as the concentration that reaches three standard deviations above a blank) is 9 ± 1 nM, above which we observe a concentration-dependent, approximately linear increase in the signal up to 130 nM (Figure 3B). We note here that such sensitivity, obtained without any amplification step, appears well suited for immunotherapy-monitoring applications where the expected serum concentration of therapeutic monoclonal antibodies reaches a high nanomolar range.³⁶ Control experiments using other non-specific antibodies or an anti-Dig Fab fragment containing only a single binding site produce signals indistinguishable from those of target-free samples (Figure 3C). Control experiments employing an antigen-conjugated strand and a second strand lacking the antigen likewise support the antibody-induced colocalization mechanism proposed, as no measurable signal change is observed under these conditions (Figure 3D, Split_ctrl#1 and #2). Of note, the approach is quite convenient: in each of the abovementioned studies, the reaction between the antibody-responsive circuit and the sample was performed in a single Eppendorf tube for 30 min (longer times do not produce significantly higher signals, Figure S3) and then transferred to the disposable electrode surface for quantification (Figure 1C).

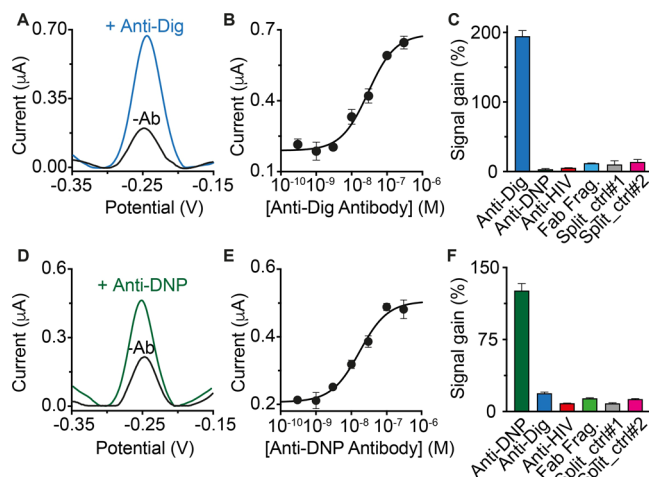


Figure 3. (A) SWV voltammograms obtained in the absence (black) and presence (blue) of anti-Dig antibodies using the optimized anti-Dig-responsive DNA circuit. (B) Current peak values obtained at increasing concentrations of anti-Dig antibodies. (C) Signal gain values observed at saturating concentration (300 nM) of anti-Dig antibodies, with non-specific antibodies and with different control experiments. Signal gain values are calculated as the relative signal change compared to the blank ($-Ab$) current signal. (D) SWV voltammograms, (E) dose–response curve, and (F) specificity tests obtained using a DNA-based circuit responsive to anti-DNP antibodies. The experiments were performed in a 100 μ L solution containing 90% bovine serum and 10% buffer solution (500 mM Na_2HPO_4 and 1.5 M NaCl at pH 7.0). The solution also contains the pre-hybridized DNA duplex (60 nM), Dig/DNP-conjugated DNA strands (100 nM each), and anti-Dig/anti-DNP antibodies (300 nM). The antibody-responsive circuits were allowed to react for 30 min at RT and then transferred to the disposable electrode surface. SWV scans were performed between -0.35 and -0.15 V at 50 Hz after 120 min from the transfer of the solution on the electrode.

The antibody-detecting DNA circuit is generalizable to the detection of other antibodies via the simple expedient of changing the employed recognition element. To demonstrate this, we engineered an antibody-controlled circuit for the detection of anti-DNP antibodies. This circuit, also, detects its target with specificity and detection limits comparable to those we found for the detection of the anti-Dig (Figure 3D–F).

The majority of clinically relevant antibodies recognize proteins, and thus, we have also adapted the circuit to the detection of peptide epitope-recognizing antibodies. To reduce the cost of synthesizing the necessary antigen-modified DNA strands, we designed a modular version of the antibody-responsive circuit that allows the use of a single antigen-conjugated strand that hybridizes to two unmodified scaffold DNA strands (one of which contains a frame inversion), thus affording a more modular platform (Figure 4A). We also employed PNA, rather than DNA, as this is easier to conjugate a peptide to it. To demonstrate utility in the detection of peptide epitope-recognizing antibodies, we have characterized sensors displaying three clinically relevant peptide antigens: a 12-residue peptide excised from the epidermal growth factor receptor and recognized by cetuximab (a monoclonal antibody used as a therapeutic drug),³⁶ a 13-residue epitope excised from the HIV protein p17 and recognized by anti-HIV antibodies,³⁷ and a 9-residue epitope excised from the human influenza hemagglutinin (HA) protein and recognized by anti-HA antibodies.³⁸ For all these electrochemical circuits, we

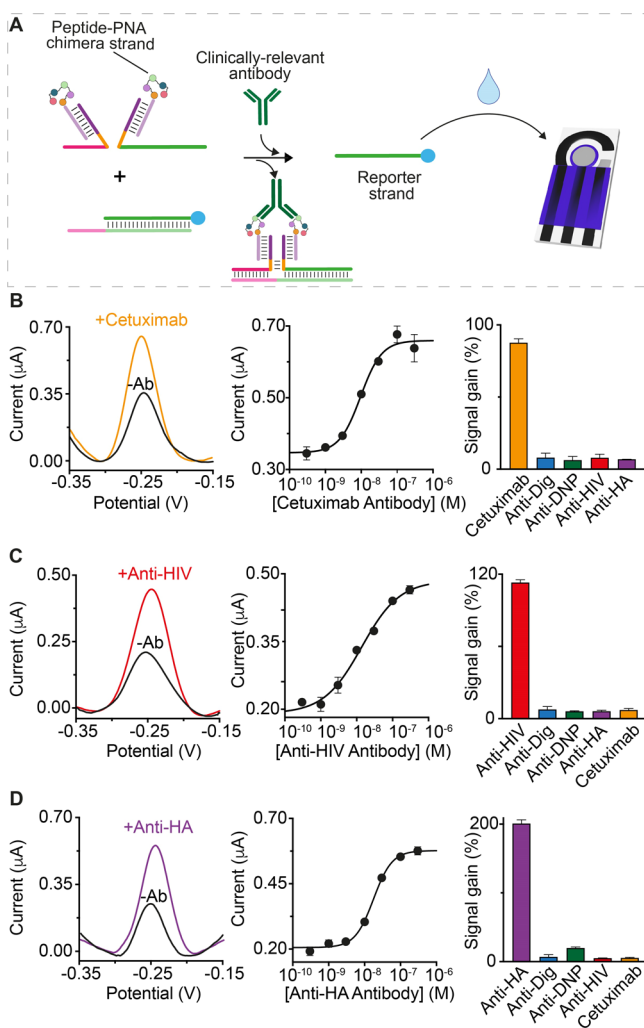


Figure 4. (A) Modular design of the electrochemical platform for the detection of three different clinically relevant antibodies: (B) cetuximab, (C) anti-HIV, and (D) anti-HA antibodies. Shown are (left) the SWV voltammograms recorded in the absence (blank) and presence (colored) of the target antibody, (center) the dose–response curves, and (right) the signal gain values obtained with the specificity tests. The experiments were performed in a 100 μL solution containing 90% bovine serum and 10% phosphate buffer (500 mM Na_2HPO_4 and 1.5 M NaCl at pH 7.0). Each solution also contains the pre-hybridized DNA duplex (60 nM), the scaffold DNA strands (60 nM each), and the peptide-PNA chimera (120 nM) and cetuximab/anti-HIV/anti-HA antibodies. Both the SWV examples and the specificity tests were performed at saturating concentrations of the target antibody (300 nM). The same experimental procedure described in Figure 3 was employed.

achieved sensitivities and specificities comparable to those of the non-modular platforms (Figure 4B–D).

The antibody-responsive DNA circuit also supports the simultaneous measurement of multiple antibodies in a single sample solution. To demonstrate this, we immobilized two distinct capture probes on one electrode. These were designed to hybridize the reporter strands of orthogonal antibody-responsive circuits for the detection of anti-Dig antibodies and cetuximab and modified with the redox reporters methylene blue and anthraquinone, respectively (Figure 5A). As the redox potentials of these reporters do not overlap, this allows the two strands to be monitored independently. The two circuits were mixed in the same Eppendorf tube and challenged with various

combinations of their target antibodies. As expected, each responds to its specific antibody, generating a separated faradic current peak, and only in the presence of both antibodies, we achieved the two current peaks corresponding to the two circuits employed (Figure 5B).

CONCLUSIONS

We have developed an electrochemical DNA circuit that responds quantitatively to multiple specific antibodies. The approach is sensitive (low nanomolar detection limit), specific (no signal is observed in the presence of non-targeted antibodies), and selective (the platform can be employed in complex media, including 90% serum). It is also versatile: this preliminary study has already demonstrated the detection of five different antibodies, including three of which are clinically important and are detectable at clinically relevant concentrations. The average serum levels of cetuximab during treatment, for example, are in the high nanomolar range.³⁶ Finally, the antibody-responsive circuit is easily multiplexed: via the use of distinct redox reporters, circuits responding to different antibodies can be employed in the same solution without significant crosstalk.

The use of synthetic DNA oligonucleotides coupled with electrochemical detection affords potentially significant benefits for antibody detection compared to optical-based approaches. First, the platform is reagentless and convenient. The antibody-responsive circuit can be completed, for example, in 30 min in a single Eppendorf tube and then simply transferred to the surface of a disposable sensor. Second, compared to optical/colorimetric approaches,^{39,40} our electrochemical platform appears better suited for use in complex clinical sample matrices without any dilution or washing step and works well even in 90% serum. Finally, the portability and low cost of electrochemical instrumentation and the cost effectiveness of disposable electrodes render electrochemical approaches easily adaptable to point-of-care formats.²² Given these attributes, we believe that the electrochemical antibody-responsive circuits we have presented may prove to be well positioned for adaptation to point-of-care diagnostics.

MATERIALS AND METHODS

Chemicals. Reagent-grade chemicals [sodium chloride (NaCl), magnesium chloride (MgCl_2), disodium hydrogen phosphate (Na_2HPO_4), 6-mercapto-1-hexanol ($\text{HS}(\text{CH}_2)_6\text{OH}$), Tris(2-carboxyethyl)phosphine (TCEP) ($\text{C}_9\text{H}_{15}\text{O}_6\text{P}$)], fetal bovine serum, and mouse monoclonal anti-DNP antibodies were purchased from Sigma-Aldrich (St Louis, Missouri) and used without further purifications. Sheep polyclonal anti-Dig antibodies, the anti-Dig Fab fragment, and anti-HA antibodies were purchased from Roche Diagnostic Corporation (Germany), anti-DNP Fab fragments were purchased from Creative Biolabs, USA, murine monoclonal anti-HIV antibodies were purchased from Zeptomatrix Corporation, and cetuximab antibodies were obtained from Merck (Darmstadt, Germany). All the antibodies were aliquoted and stored at 4 °C for immediate use or at 20 °C for long-term storage. Substrates used for printing electrodes (polyesters, Autostat HTS, $d = 0.175$ mm) were purchased from Autotype, Milan. Inks were delivered by Henkel (Milan) and were of different types: Elettrodag PF497A based on graphite; Elettrodag PF410 based on silver; and Elettrodag 6018SS for the insulator.

Preparation of DNA-Modified Electrodes. The DNA capture probe (100 μM) was reduced for 1 h in a solution of 0.4 mM Tris(2-carboxyethyl)phosphine hydrochloride (TCEP) prepared in 150 mM NaCl and 50 mM NaH_2PO_4 , pH 7.0, to allow reduction of disulfide

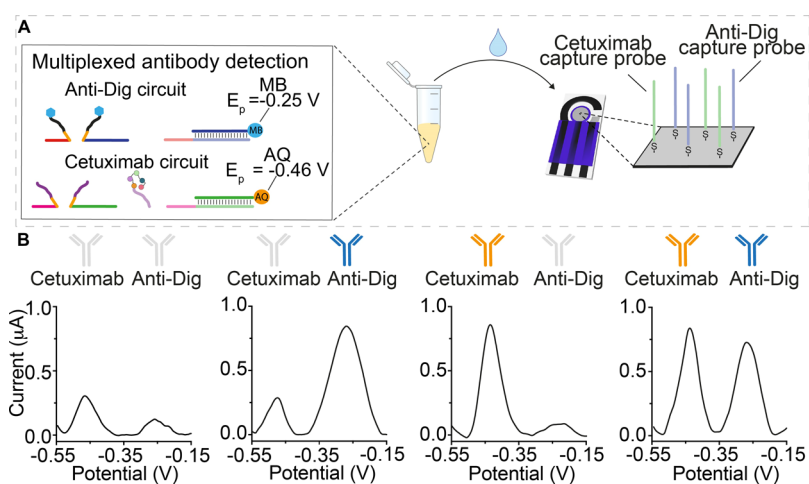


Figure 5. (A) Multiplex detection of anti-Dig (blue) and cetuximab (orange) antibodies using two orthogonal-responsive circuits releasing two different reporter strands labeled with two non-interfering redox labels (i.e., methylene blue, MB, and anthraquinone, AQ). (B) SWV profiles achieved for different experiments performed in the absence of both antibodies (left), in the presence of only one antibody (center), and in the presence of both antibodies (right). The colored antibody image identifies the added target for each experiment. The experiments were performed in a 100 μL phosphate buffer (50 mM Na_2HPO_4 , 150 mM NaCl, pH 7.0) solution containing the two antibody-responsive circuits as previously described. The SWV voltammograms were obtained at saturating concentrations of the target antibody (300 nM).

bonds. This solution was diluted to a final concentration of 100 nM in the same buffer. The DNA capture probe (20 μL) was dropcast only onto the silver working electrode of the SPE. After 1 h of incubation, SPE was rinsed with water, and 20 μL of 2 mM mercaptohexanol (prepared in 150 mM NaCl, 50 mM Na_2HPO_4 , pH 7.0) was dropcast only onto the WE of the SPE to displace non-specifically adsorbed DNA and passivate the electrode area. After 1.5 h of incubation, SPE was rinsed with water.

Oligonucleotides and DNA Circuits. HPLC-purified oligonucleotides were purchased from IBA (Göttingen, Germany) or Biosearch Technologies (Risskov, Denmark). All the DNA sequences used in this work are reported in the [Supporting Information](#) document.

Electrochemical Experiments. All electrochemical measurements were performed at room temperature using an EmStatMUX potentiostat multiplexer (Palmsens Instruments, Netherland). The Ab-responsive circuits were allowed to react in an Eppendorf tube for 30 min at RT and then transferred to the disposable electrode surface. Experimental data were collected using square wave voltammetry from -0.15 to -0.35 V in increments of 0.001 V versus Ag/AgCl, with an amplitude of 10 mV and a frequency of 50 Hz for when using methylene blue as a redox label. Square wave voltammetry for the circuit that employs anthraquinone was performed from -0.1 to -0.55 V in increments of 1 mV versus Ag/AgCl, with an amplitude of 50 mV and a frequency of 50 Hz. Peak currents were fit using the manual fit mode in PSTrace 4.5v software (of Palmsens Instrument). All experiments were performed in a 100 μL phosphate 50 mM Na_2HPO_4 , 150 mM NaCl, pH 7.0 solution at 25 $^\circ\text{C}$.

Data Analysis. Binding curves were fit with the following four-parameter logistic equation

$$i[\text{Ab}] = i_0 + (i_{\text{Ab}} - i_0) \times \frac{[\text{Ab}]^{\text{nH}}}{[\text{Ab}]^{\text{nH}} + K_{1/2}^{\text{nH}}}$$

where $i[\text{Ab}]$ is the current observed in the presence of a given concentration of the target analyte; i_0 is the background current observed in the absence of the target analyte; $[\text{Ab}]$ is the antibody concentration; i_{Ab} is the current seen in the presence of saturating concentration of the target; $K_{1/2}$ is the concentration at half of the maximum signal change; and nH is the Hill coefficient. Signal gain (%) values used to compare specificity experiments are calculated as the relative signal change registered upon the addition of saturating concentration of target antibodies (or non-specific antibodies) using the following formula

$$\text{signal gain (\%)} = \frac{i_{\text{Ab}} - i_0}{i_0} \times 100$$

where i_{Ab} = current in the presence of different concentrations of the antibody; i_0 = background current. The limit of detection (LOD) was determined as the concentration that reaches three standard deviations above a blank.

■ ASSOCIATED CONTENT

Supporting Information

The Supporting Information is available free of charge at <https://pubs.acs.org/doi/10.1021/acssensors.1c00790>.

DNA circuit sequences and electrochemical kinetic traces of the anti-Dig-responsive circuit ([PDF](#))

■ AUTHOR INFORMATION

Corresponding Authors

Simona Ranallo – Department of Chemical Science and Technologies, University of Rome, Tor Vergata, 00133 Rome, Italy; Department of Chemistry and Biochemistry, University of California Santa Barbara, CA93106 Santa Barbara, California, United States; Email: simona.ranallo@uniroma2.it

Francesco Ricci – Department of Chemical Science and Technologies, University of Rome, Tor Vergata, 00133 Rome, Italy; orcid.org/0000-0003-4941-8646; Email: francesco.ricci@uniroma2.it

Authors

Sara Bracaglia – Department of Chemical Science and Technologies, University of Rome, Tor Vergata, 00133 Rome, Italy

Kevin W. Plaxco – Department of Chemistry and Biochemistry, University of California Santa Barbara, CA93106 Santa Barbara, California, United States;

orcid.org/0000-0003-4772-8771

Complete contact information is available at:

<https://pubs.acs.org/doi/10.1021/acssensors.1c00790>

Author Contributions

S.R., K.W.P., and F.R. conceived and designed the experiments; S.B. and S.R. performed the experiments; S.B., S.R., K.W.P., and F.R. analyzed the data; S.R., K.W.P., and F.R. wrote the paper.

Notes

The authors declare no competing financial interest.

ACKNOWLEDGMENTS

This work received funding from the European Union's Horizon 2020 research and innovation program under the Marie Skłodowska-Curie grant agreement n. 843179 ("DNA-NANO-AB", S.R.). The work was also supported by Associazione Italiana per la Ricerca sul Cancro, AIRC (project n. 21965, F.R.) and by the European Research Council, ERC (Consolidator Grant project n. 819160, F.R.).

REFERENCES

- (1) Taleghani, N.; Taghipour, F. Diagnosis of COVID-19 for Controlling the Pandemic: A Review of the State-of-the-Art. *Biosens. Bioelectron.* **2021**, *174*, 112830.
- (2) Bhalla, N.; Pan, Y.; Yang, Z.; Payam, A. F. Opportunities and Challenges for Biosensors and Nanoscale Analytical Tools for Pandemics: COVID-19. *ACS Nano* **2020**, *14*, 7783–7807.
- (3) Urdea, M.; Penny, L. A.; Olmsted, S. S.; Giovanni, M. Y.; Kaspar, P.; Shepherd, A.; Wilson, P.; Dahl, C. A.; Buchsbaum, S.; Moeller, G.; Hay Burgess, D. C. Requirements for High Impact Diagnostics in the Developing World. *Nature* **2006**, *444*, 73–79.
- (4) Remais, J. V.; Zeng, G.; Li, G.; Tian, L.; Engelgau, M. M. Convergence of Non-Communicable and Infectious Diseases in Low- and Middle-Income Countries. *Int. J. Epidemiol.* **2013**, *42*, 221–227.
- (5) Robbins, A.; Hentzien, M.; Toquet, S.; Didier, K.; Servettaz, A.; Pham, B.-N.; Giusti, D. Diagnostic Utility of Separate Anti-Ro60 and Anti-Ro52/TRIM21 Antibody Detection in Autoimmune Diseases. *Front. Immunol.* **2019**, *10*, 444.
- (6) Fortner, R. T.; Damms-Machado, A.; Kaaks, R. Systematic Review: Tumor-Associated Antigen Autoantibodies and Ovarian Cancer Early Detection. *Gynecol. Oncol.* **2017**, *147*, 465–480.
- (7) Ludwig, J. A.; Weinstein, J. N. Biomarkers in Cancer Staging, Prognosis and Treatment Selection. *Nat. Rev. Cancer* **2005**, *5*, 845–856.
- (8) Vieira, P. A.; Shin, C. B.; Arroyo-Currás, N.; Ortega, G.; Li, W.; Keller, A. A.; Plaxco, K. W.; Kippin, T. E. Ultra-High-Precision, in-Vivo Pharmacokinetic Measurements Highlight the Need for and a Route Toward More Highly Personalized Medicine. *Front. Mol. Biosci.* **2019**, *6*, 69.
- (9) Fesnak, A. D.; June, C. H.; Levine, B. L. Engineered T Cells: The Promise and Challenges of Cancer Immunotherapy. *Nat. Rev. Cancer* **2016**, *16*, 566–581.
- (10) Krishnamurthy, A.; Jimeno, A. Bispecific Antibodies for Cancer Therapy: A Review. *Pharmacol. Ther.* **2018**, *185*, 122–134.
- (11) Nayak, S.; Blumenfeld, N. R.; Laksanasopin, T.; Sia, S. K. Point-of-Care Diagnostics: Recent Developments in a Connected Age. *Anal. Chem.* **2017**, *89*, 102–123.
- (12) Wood, C. S.; Thomas, M. R.; Budd, J.; Mashamba-Thompson, T. P.; Herbst, K.; Pillay, D.; Peeling, R. W.; Johnson, A. M.; McKendry, R. A.; Stevens, M. M. Taking Connected Mobile-Health Diagnostics of Infectious Diseases to the Field. *Nature* **2019**, *566*, 467–474.
- (13) Brangel, P.; Sobarzo, A.; Parolo, C.; Miller, B. S.; Howes, P. D.; Gekop, S.; Lutwama, J. J.; Dye, J. M.; McKendry, R. A.; Lobel, L.; Stevens, M. M. A Serological Point-of-Care Test for the Detection of IgG Antibodies against Ebola Virus in Human Survivors. *ACS Nano* **2018**, *12*, 63–73.
- (14) Loynachan, C. N.; Thomas, M. R.; Gray, E. R.; Richards, D. A.; Kim, J.; Miller, B. S.; Brookes, J. C.; Agarwal, S.; Chudasama, V.; McKendry, R. A.; Stevens, M. M. Platinum Nanocatalyst Amplifica-

tion: Redefining the Gold Standard for Lateral Flow Immunoassays with Ultrabroad Dynamic Range. *ACS Nano* **2018**, *12*, 279–288.

(15) Wang, D.; He, S.; Wang, X.; Yan, Y.; Liu, J.; Wu, S.; Liu, S.; Lei, Y.; Chen, M.; Li, L.; Zhang, J.; Zhang, L.; Hu, X.; Zheng, X.; Bai, J.; Zhang, Y.; Zhang, Y.; Song, M.; Tang, Y. Rapid Lateral Flow Immunoassay for the Fluorescence Detection of SARS-CoV-2 RNA. *Nat. Biomed. Eng.* **2020**, *4*, 1150–1158.

(16) Teymourian, H.; Barfidokht, A.; Wang, J. Electrochemical glucose sensors in diabetes management: An updated review (2010–2020). *Chem. Soc. Rev.* **2020**, *49*, 7671–7709.

(17) Dai, Y.; Liu, C. C. Recent Advances on Electrochemical Biosensing Strategies toward Universal Point-of-Care Systems. *Angew. Chem. Int. Ed.* **2019**, *58*, 12355–12368.

(18) Wouters, S. F. A.; Wijker, E.; Merckx, M. Optical Control of Antibody Activity by Using Photocleavable Bivalent Peptide-DNA Locks. *ChemBioChem.* **2019**, *20*, 2463–2466.

(19) Tomimuro, K.; Tenda, K.; Ni, Y.; Hiruta, Y.; Merckx, M.; Citterio, D. Thread-Based Bioluminescent Sensor for Detecting Multiple Antibodies in a Single Drop of Whole Blood. *ACS Sens.* **2020**, *5*, 1786–1794.

(20) Engelen, W.; Meijer, L. H. H.; Somers, B.; De Greef, T. F. A.; Merckx, M. Antibody-controlled actuation of DNA-based molecular circuits. *Nat. Commun.* **2017**, *8*, 14473.

(21) Rossetti, M.; Brannetti, S.; Mocenigo, M.; Marini, B.; Ippodrino, R.; Porchetta, A. Harnessing Effective Molarity to Design an Electrochemical DNA-based Platform for Clinically Relevant Antibody Detection. *Angew. Chem. Int. Ed.* **2020**, *59*, 14973–14978.

(22) Labib, M.; Sargent, E. H.; Kelley, S. O. Electrochemical Methods for the Analysis of Clinically Relevant Biomolecules. *Chem. Rev.* **2016**, *116*, 9001–9090.

(23) Pei, H.; Lu, N.; Wen, Y.; Song, S.; Liu, Y.; Yan, H.; Fan, C. A DNA Nanostructure-Based Biomolecular Probe Carrier Platform for Electrochemical Biosensing. *Adv. Mater.* **2010**, *22*, 4754–4758.

(24) Chen, X.; Zhou, G.; Song, P.; Wang, J.; Gao, J.; Lu, J.; Fan, C.; Zuo, X. Ultrasensitive Electrochemical Detection of Prostate-Specific Antigen by Using Antibodies Anchored on a DNA Nanostructural Scaffold. *Anal. Chem.* **2014**, *86*, 7337–7342.

(25) Pei, H.; Wan, Y.; Li, J.; Hu, H.; Su, Y.; Huang, Q.; Fan, C. Regenerable Electrochemical Immunological Sensing at DNA Nanostructure-Decorated Gold Surfaces. *Chem. Commun.* **2011**, *47*, 6254–6256.

(26) Mahshid, S. S.; Mahshid, S.; Vallée-Bélisle, A.; Kelley, S. O. Peptide-Mediated Electrochemical Steric Hindrance Assay for One-Step Detection of HIV Antibodies. *Anal. Chem.* **2019**, *91*, 4943–4947.

(27) Das, J.; Gomis, S.; Chen, J. B.; Yousefi, H.; Ahmed, S.; Mahmud, A.; Zhou, W.; Sargent, E. H.; Kelley, S. O. Reagentless Biomolecular Analysis Using a Nanoscale Molecular Pendulum. *Nat. Chem.* **2021**, *13*, 428–434.

(28) Arter, W. E.; Yusim, Y.; Peter, Q.; Taylor, C. G.; Klenerman, D.; Keyser, U. F.; Knowles, T. P. J. Digital Sensing and Molecular Computation by an Enzyme-Free DNA Circuit. *ACS Nano* **2020**, *14*, 5763–5771.

(29) Yue, L.; Wang, S.; Wulf, V.; Lilienthal, S.; Remacle, F.; Levine, R. D.; Willner, I. Consecutive feedback-driven constitutional dynamic networks. *Proc. Natl. Acad. Sci. U.S.A.* **2019**, *116*, 2843–2848.

(30) Ranallo, S.; Sorrentino, D.; Ricci, F. Orthogonal Regulation of DNA Nanostructure Self-Assembly and Disassembly Using Antibodies. *Nat. Commun.* **2019**, *10*, 5509.

(31) Jung, C.; Ellington, A. D. Diagnostic applications of nucleic acid circuits. *Acc. Chem. Res.* **2014**, *47*, 1825–1835.

(32) Wang, H.; Wang, H.; Willner, I.; Wang, F. High-performance biosensing based on autonomous enzyme-free DNA circuits. *Top. Curr. Chem.* **2020**, *378*, 20.

(33) Orbach, R.; Willner, B.; Willner, I. Catalytic nucleic acids (DNazymes) as functional units for logic gates and computing circuits: from basic principles to practical applications. *Chem. Commun.* **2015**, *51*, 4144–4160.

(34) Sadat Mousavi, P.; Smith, S. J.; Chen, J. B.; Karlikow, M.; Tinifar, A.; Robinson, C.; Liu, W.; Ma, D.; Green, A. A.; Kelley, S. O.;

Pardee, K. A multiplexed, electrochemical interface for gene-circuit-based sensors. *Nat. Chem.* **2020**, *12*, 48–55.

(35) Ranallo, S.; Porchetta, A.; Ricci, F. DNA-Based Scaffolds for Sensing Applications. *Anal. Chem.* **2019**, *91*, 44–59.

(36) Robert, F.; Ezekiel, M. P.; Spencer, S. A.; Meredith, R. F.; Bonner, J. A.; Khazaeli, M. B.; Saleh, M. N.; Carey, D.; LoBuglio, A. F.; Wheeler, R. H.; Cooper, M. R.; Waksal, H. W. Phase I Study of Anti-Epidermal Growth Factor Receptor Antibody Cetuximab in Combination With Radiation Therapy in Patients With Advanced Head and Neck Cancer. *J. Clin. Oncol.* **2001**, *19*, 3234–3243.

(37) Papsidero, L. D.; Sheu, M.; Ruscetti, F. W. Human Immunodeficiency Virus Type 1-Neutralizing Monoclonal Antibodies Which React with P17 Core Protein: Characterization and Epitope Mapping. *J. Virol.* **1989**, *63*, 267–272.

(38) Fleury, D.; Wharton, S. A.; Skehel, J. J.; Knossow, M.; Bizebard, T. Antigen Distortion Allows Influenza Virus to Escape Neutralization. *Nat. Struct. Biol.* **1998**, *5*, 119–123.

(39) Ranallo, S.; Rossetti, M.; Plaxco, K. W.; Vallée-Bélisle, A.; Ricci, F. A Modular, DNA-Based Beacon for Single-Step Fluorescence Detection of Antibodies and Other Proteins. *Angew. Chem. Int. Ed.* **2015**, *54*, 13214–13218.

(40) Mocenigo, M.; Porchetta, A.; Rossetti, M.; Brass, E.; Tonini, L.; Puzzi, L.; Tagliabue, E.; Triulzi, T.; Marini, B.; Ricci, F.; Ippodrino, R. Rapid, Cost-Effective Peptide/Nucleic Acid-Based Platform for Therapeutic Antibody Monitoring in Clinical Samples. *ACS Sens.* **2020**, *5*, 3109–3115.